Structural Engineering and Mechanics, Vol. 4, No. 2 (1996) 111-124
DOI: http://dx.doi.org/10.12989/sem.1996.4.2.111

Spatially filtered multi-field responses of piezothermoelastic cylindrical shell composites

H. S. Tzou† and Y. Bao‡

Department of Mechanical Engineering, Center for Manufacturing Systems, University of Kentucky, Lexington, Kentucky 40506-0108, U.S.A.

Abstract. New active "intelligent" structural systems with integrated self-sensing, diagnosis, and control capabilities can lead to a new design dimension for the next generation high-performance structures and mechanical systems. However, temperature effects to the piezoelectric transducers are not fully understood. This paper is concerned with a mathematical modeling and analysis of a laminated piezothermoelastic cylindrical shell composite exposed to mechanical, electric, and thermal fields. Generic shell equations and solution procedures are derived. Contributions of spatial and time components in the mechanical, electric, and temperature excitations are discussed, and their analytical solutions derived. A laminated cylindrical shell composite with fully distributed piezoelectric layers is used in a case study; its multi-field step and impulse responses are investigated. Analyses suggest that the fully distributed actuators are insensitive to even modes due to load averaging and cancellation. Accordingly, these even modes are filtered from the total response and only the modes that are combinations of $m=1, 3, 5, \cdots$ and $n=1, 3, 5, \cdots$ participating in dynamic response of the shell.

Key words: piezoelectric transducers; smart structures; distributed control

1. Introduction

New active "intelligent" structural systems with integrated sensing, diagnosis, and control capabilities can lead to a new design dimension for the next generation high-performance structural and mechanical systems (Tzou and Anderson 1992, Tzou and Fukuda 1992). Piezoelectrics have inherent electromechanical characterisitics: *the direct and converse piezoelectric effects,* and they are very popular in both sensor and actuator applications in intelligent structural systems (Tzou 1993). Distributed sensing and control of elastic and composite continua using distributed piezoelectric transducers has been studied recently. However, temperature effects to these distributed sensors/actuators are not well understood. Depending on piezoelectric properties, temperature fluctuation can significantly change the sensing and control effects of distributed piezoelectric transducers. Mindlin (1974) derived governing equations of a linear piezothermoelastic medium. Nowacki (1978) proposed a uniqueness theorem for the solutions of piezothermoelastic differential equations. Nowacki (1982) discussed the influence of a temperature field on an elastic dielectric medium and a reciprocity theorem. Tzou and Howard (1994a, 1994b) proposed a piezothermo-

† Professor
‡ Ph.D Candidate

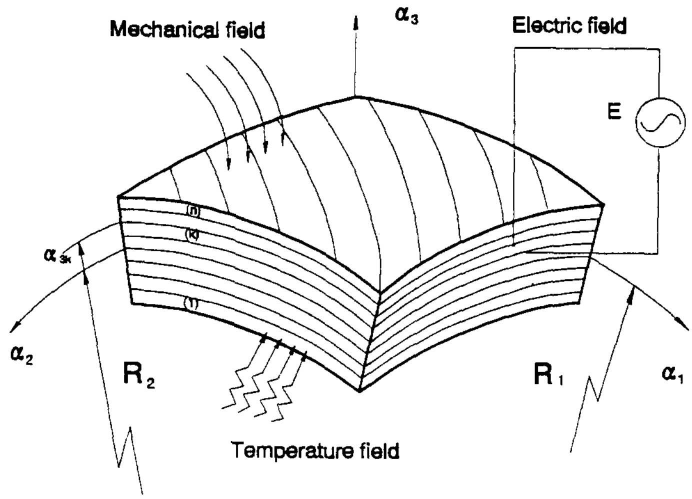

Fig. 1 A generic piezothermoelastic shell.

elastic shell vibration theory with applications to active ring shells. Tzou and Ye (1994) studied the thermal influence to distributed transducers and investigated thermoelectromechanical characteristics and static/vibration control of structures. This paper is concerned with a mathematical modeling and analysis of a laminated piezothermoelastic shell composite exposed to mechanical, electric, and thermal fields. Generic solution procedures are derived and applied to a laminated cylindrical shell composite with distributed mechanical, electric, and thermal excitations. A numerical example is provided to illustrate the multi-field step and impulse responses. Spatially filtered modal responses are also investigated.

2. Multi-field excitation and response

It is assumed that a double-curvature piezothermoelastic shell is exposed to three fields: mechanical, electric, and temperature fields, Fig. 1. Note that the shell is defined in a curvilinear coordinate system with α_1 and α_2 defining the neutral (or reference) surface and α_3 the normal direction. In this section, multi-field step and impulse responses of a piezothermoelastic shell is discussed and solution procedures derived.

A simplified piezothermoelastic shell equation with mechanical, electric, and temperature excitations can be expressed as

$$L_i^m\{u_1,\ u_2,\ u_3\}+L_i^d\{u_1,\ u_2,\ u_3\}-c\dot{u}_i-\rho h\ddot{u}_i=-q_i^*,\ i=1,\ 2,\ 3, \tag{1}$$

where i denotes the i-th direction; u_i, $\dot{u}_i$, and $\ddot{u}_i$ are displacement, velocity, and acceleration, respectively; $L_i^m\{u_1,\ u_2,\ u_3\}$ is a Love's operator of the mechanical effect; $L_i^d\{u_1,\ u_2,\ u_3\}$ is an operator of the direct piezoelectric effect; c is an equivalent viscous damping factor; ρ is the weighted mass density; h is the shell thickness; $c\dot{u}_i$ is the viscous damping force; $\rho h\ddot{u}_i$ is the inertia force; and q_i^* is the generalized force, $q_i^*=q_i+L_i^c(\phi_3)+L_i^p(\theta)+L_i^\theta(\theta)$. In the generalized force, q_i is the distributed external mechanical forces; $L_i^c(\phi_3)$ is an operator of the converse piezoelectric effect; $L_i^p(\theta)$ is an operator of the pyroelectric effect; and $L_i^\theta(\theta)$ is an operator of the thermal strain (expansion and contraction) effect (Tzou and Bao 1995a, Tzou and Ye 1994). Detailed definitions of these operators are presented in Appendix.

The response of the piezothermoelastic shell subjected to mechanical, electric, and temperature excitations can be represented by a summation of all participating natural modes-the modal expansion method. The amount of participation of each natural mode in the total response is defined by the modal participation factor. Thus, the general solution of the piezothermoelastic shell continuum can be represented by an infinite series of shell's eigenfunctions in the form (Soedel 1993, Tzou 1993):

$$u_i(\alpha_1, \alpha_2, t)=\sum_{k=1}^{\infty} \eta_k(t)U_{ik}(\alpha_1, \alpha_2),\ i=1, 2, 3, \tag{2}$$

where $\eta_k(t)$ is the modal participation factor and $U_{ik}(\alpha_1, \alpha_2)$ is the natural mode function (mode shape function) in the i-th directions ($i=1, 2, 3$). Substituting the expressions of u_i into the governing equation and using the modal orthogonality, one can derive the k-th modal participation factor equation-the modal equation:

$$\ddot{\eta}_k+\frac{c}{\rho h}\dot{\eta}_k+\omega_k^2\eta_k=F_k, \tag{3}$$

where ω_k is the (undamped) natural frequency; $F_k=F_k^m+F_k^c+F_k^t$ is the generalized modal force for the k-th mode. F_k^m, F_k^c, and F_k^t are respectively the generalized mechanical, electric, and thermal modal forces defined by

$$F_k^m=\frac{1}{\rho h N_k}\int_{\alpha_1}\int_{\alpha_2}\sum_{i=1}^{3}[q_i U_{ik}]A_1A_2d\alpha_1 d\alpha_2, \tag{4a}$$

$$F_k^c=\frac{1}{\rho h N_k}\int_{\alpha_1}\int_{\alpha_2}\sum_{i=1}^{3}[L_i^c(\phi_3)U_{ik}]A_1A_2d\alpha_1 d\alpha_2, \tag{4b}$$

$$F_k^t=\frac{1}{\rho h N_k}\int_{\alpha_1}\int_{\alpha_2}\sum_{i=1}^{3}\{[L_i^p(\theta)+L_i^\theta(\theta)]U_{ik}\}A_1A_2d\alpha_1 d\alpha_2, \tag{4c}$$

where A_1 and A_2 are the Lamé parameters and N_k is defined by the mode shape functions: $N_k=\int_{\alpha_1}\int_{\alpha_2}(\sum_{i=1}^{3}U_{ik}^2)\ A_1A_2d\alpha_1\alpha_2$ (Soedel 1993, Tzou 1993). Introducing a (modal viscous) damping ratio $\zeta_k=\frac{c}{2\rho h\omega_k}$, one can rewrite the modal equation as

$$\ddot{\eta}_k+2\zeta_k\omega_k\dot{\eta}_k+\omega_k^2\eta_k=F_k. \tag{5}$$

Since the piezothermoelastic shell is assumed linear, the principle of superposition is valid. Thus, each modal participation factor can be solved independently and the overall shell response can be determined by the modal expansion equation, Eq.(2). Detailed multi-field responses of a laminated cylindrical shell composite are presented next.

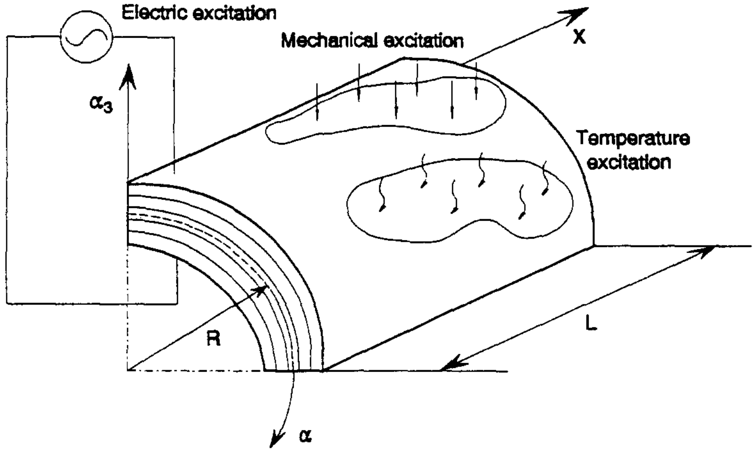

Fig. 2 A laminated cylindrical shell.

3. Laminated cylindrical shell composite

A laminated cylindrical shell is made of five laminae: three graphite/epoxy laminae with 90°/0°/90° lamination sandwiched between two piezoelectric laminae on the top and bottom surfaces (Tzou and Bao 1995b). Fig. 2 illustrates the laminate cylindrical shell. In this section, detailed multi-field responses are analyzed. Numerical solutions are presented in the next section.

Note that the cylindrical shell is defined by a radius R, length L, and curvature angle β. For a simply supported laminated cylindrical shell compoiste, the transverse mode shape function is $U_{3mn}=C_{imn}\sin\left(\frac{m\pi x}{L}\right)\sin\left(\frac{n\pi\alpha}{\beta}\right)$ where m and n are the half-wave mode numbers; L is the length; β is the curvature angle; and C_{imn} is an arbitrary constant. Accordingly, N_{mn} can be defined by

$$N_{mn}=\int_0^L\int_0^\beta\left(\sum_{i=1}^{3}U_{imn}^2\right)R\,d\alpha\,dx\simeq\int_0^L\int_0^\beta\sin^2\left(\frac{m\pi x}{L}\right)\sin^2\left(\frac{n\pi\alpha}{\beta}\right)R\,d\alpha\,dx=\frac{RL\beta}{4} \tag{6}$$

The generalized mechanical, electric, and thermal modal forces are

$$F_{mn}^m=\frac{4}{\rho hL\beta}\int_0^L\int_0^\beta q_3\sin\left(\frac{m\pi x}{L}\right)\sin\left(\frac{n\pi\alpha}{\beta}\right)d\alpha\,dx, \tag{7}$$

$$\begin{aligned}F_{mn}^c=\frac{4}{\rho hL\beta}\int_0^L\int_0^\beta\Bigg\{&\left[\frac{e_{31}}{2}(h_1+3h_2)\frac{\partial^2}{\partial x^2}(\phi_{35}^c-\phi_{31}^c)\right]\\&+\left[\frac{e_{31}}{2R^2}(h_1+3h_2)\frac{\partial_2}{\partial\alpha^2}(\phi_{35}^c-\phi_{31}^c)\right]-\left[\frac{e_{31}}{R}(\phi_{31}^c+\phi_{35}^c)\right]\Bigg\}\sin\left(\frac{m\pi x}{L}\right)\sin\left(\frac{n\pi\alpha}{\beta}\right)d\alpha\,dx,\end{aligned} \tag{8}$$

$$\begin{aligned}F_{mn}^t=\frac{4}{\rho hL\beta}\int_0^L\int_0^\beta\Bigg\{&\left[\left(\frac{e_{31}p_3}{\varepsilon_{33}}\right)\sum_{k=1,5}\int_{\alpha_{3k-1}}^{\alpha_{3k}}\frac{\partial^2\theta}{\partial x^2}\alpha_3\,d\alpha_3-\sum_{k=1}^{5}\int_{\alpha_{3k-1}}^{\alpha_{3k}}(\bar{\lambda}_1)_k\frac{\partial^2\theta}{\partial x^2}\alpha_3\,d\alpha_3\right]\\&+\frac{1}{R^2}\left[\left(\frac{e_{31}p_3}{\varepsilon_{33}}\right)\sum_{k=1,5}\int_{\alpha_{3k-1}}^{\alpha_{3k}}\frac{\partial^2\theta}{\partial\alpha^2}\alpha_3\,d\alpha_3-\sum_{k=1}^{5}\int_{\alpha_{3k-1}}^{\alpha_{3k}}(\bar{\lambda}_2)_k\frac{\partial^2\theta}{\partial\alpha^2}\alpha_3\,d\alpha_3\right]\end{aligned}$$

$$-\frac{1}{R^2}\left[\left(\frac{e_{31}p_3}{\varepsilon_{33}}\right)\sum_{k=1,5}\int_{a_{3k-1}}^{a_{3k}}\theta d\alpha_3-\sum_{k=1}^{5}\int_{a_{3k-1}}^{a_{3k}}(\bar{\lambda}_2)_k\,\theta d\alpha_3\right]\Bigg\}\sin\left(\frac{m\pi x}{L}\right)\sin\left(\frac{n\pi\alpha}{\beta}\right)d\alpha dx, \tag{9}$$

where e_{31} is the piezoeletric constant; h_i is the i-th layer thickness; ϕ_{3i} is the transverse electric field applied to the i-th layer; ε_{33} is the dielectric constant; p_3 is the pyroelectric constant; θ is the temperature rise; R is the radius; and $\bar{\lambda}_i$ is the transformed thermal stress coefficent. (In the laminated composite, $h_1=h_5$ and $h_2=h_3=h_4$) In the expressions of F^c_{mn} and F^t_{mn}, the first square bracketed component is due to the bending moment M_{xx}; the second square bracketed component is due to the bending moment $M_{\alpha\alpha}$; and the third square bracketed component is due to the membrane force $N_{\alpha\alpha}$. Note that for each generalized force, there are two important components. One is its spatial distribution, e.g., point, line, surface, etc., and the other is its time function, e.g., step, impulse, sinusoidal, etc. These modal forces and their time/spatial components are discussed below. Spatial characteristics of these forces are discussed first; the time function is assumed a step function and an impulse function in this study. Spatially filtered modal responses are also discussed.

3.1. Mechanical force

For a uniformly distributed mechanical load normal to the surface, i.e. $q_3(x, \alpha, t)\equiv q_3(t)$, the generalized mechanical modal force is

$$\begin{aligned}
F^m_{mn}&=\frac{4}{\rho hL\beta}\int_0^L\int_0^\beta q_3(t)\sin\left(\frac{m\pi x}{L}\right)\sin\left(\frac{n\pi\alpha}{\beta}\right)d\alpha dx\\
&=\frac{4}{\rho hL\beta}\frac{L}{m\pi}\frac{\beta}{n\pi}q_3(t)[(-1)^m-1][(-1)^n-1]\\
&=\begin{cases}\dfrac{16q_3(t)}{\rho h\pi^2 mn}, & \text{when } m \text{ and } n \text{ odd;}\\ 0, & \text{when } m \text{ or } n \text{ even,}\end{cases}
\end{aligned} \tag{10}$$

3.2. Electric force

For the cylindrical piezoelectric layers (the 1st and 5th layers) with fully covered electrodes, it is assumed that the excitation voltages ϕ^c_{31} and ϕ^c_{35} are uniform on the shell surface, i.e. $\phi^c_{35}=\phi_1(t)$, and $\phi^c_{35}=\phi_5(t)$. That is the electrode surface is a potential equivalent surface. Then, the generalized electric modal force becomes

$$\begin{aligned}
F^c_{mn}&=\frac{4}{\rho hL\beta}\int_0^L\int_0^\beta\left\{-\frac{e_{31}}{R}[\phi_1(t)+\phi_5(t)]\right\}\sin\left(\frac{m\pi x}{L}\right)\sin\left(\frac{n\pi\alpha}{\beta}\right)d\alpha dx\\
&=\frac{4}{\rho hL\beta}\frac{L}{m\pi}\frac{\beta}{n\pi}\left\{-\frac{e_{31}}{R}[\phi_1(t)+(\phi_5(t)]\right\}[(-1)^m-1][(-1)^n-1]\\
&=\begin{cases}-\dfrac{16}{\rho h\pi^2 mn}\dfrac{e_{31}}{R}[\phi_1(t)+\phi_5(t)], & \text{when } m \text{ and } n \text{ odd;}\\ 0, & \text{when } m \text{ or } n \text{ even,}\end{cases}
\end{aligned} \tag{11}$$

It can be seen that the above expression only has the contribution of membrane force $N_{\alpha\alpha}$ in this uniform voltage distribution. Assume $\phi_1(t)=\phi_5(t)=\phi(t)$, then,

$$F^c_{mn}=\begin{cases} -\dfrac{32e_{31}}{\rho h\pi^2 mnR}\phi(t), & \text{when } m \text{ and } n \text{ odd;} \\ 0, & \text{when } m, \text{ or } n \text{ even.} \end{cases} \tag{12}$$

3.3 Thermal force

Assume the temperature rise θ is uniform on the shell surface and linear variation through the thickness $\theta(\alpha_3, t)=(a\alpha_3+c)f(t)$ where $a=\dfrac{\theta_5-\theta_0}{2h_1+3h_2}$; $c=\dfrac{\theta_5+\theta_0}{2}$; θ_5 is the temperature rise on the top surface; θ_0 is the temperature rise on the bottom surface of the laminated shell. Since the top (5th) and bottom (1st) layers are piezoelectric materials, the temperature induced pyroelectric effect appears on these two layers. However, the thermal strain effect appears in all five layers.

$$\begin{aligned} F^t_{mn} &= \frac{4}{\rho hL\beta}\int_0^L\int_0^\beta\Bigg\{-\frac{1}{R}\Bigg[\left(\frac{e_{31}p_3}{\varepsilon_{33}}\right)\sum_{k=1,5}\int_{\alpha_{3k-1}}^{\alpha_{3k}}\theta d\alpha_3 \\ &\quad - \sum_{k=1}^{5}\int_{\alpha_{3k-1}}^{\alpha_{3k}}(\bar{\lambda}_2)_k\,\theta d\alpha_3\Bigg]\Bigg\}\sin\left(\frac{m\pi x}{L}\right)\sin\left(\frac{n\pi\alpha}{\beta}\right)d\alpha dx \\ &= \frac{4}{\rho hL\beta}\frac{L}{m\pi}\frac{\beta}{n\pi}\left[-\frac{1}{R}\widetilde{T}f(t)\right][(-1)^m-1][(-1)^n-1] \\ &= \begin{cases} -\dfrac{16\widetilde{T}f(t)}{\rho h\pi^2 mnR,} & \text{when } m \text{ and } n \text{ odd;} \\ 0, & \text{when } m \text{ or } n \text{ even,} \end{cases} \end{aligned} \tag{13}$$

where

$$\begin{aligned} \widetilde{T} &= \left(\frac{e_{31}p_3}{\varepsilon_{33}}\right)\sum_{k=1,5}\int_{\alpha_{3k-1}}^{\alpha_{3k}}(a\alpha_3+c)\,d\alpha_3-\sum_{k=1}^{5}\int_{\alpha_{3k-1}}^{\alpha_{3k}}(\bar{\lambda}_2)_k(a\alpha_3+c)\,d\alpha_3 \\ &= \left(\frac{e_{31}p_3}{\varepsilon_{33}}\right)\left[\int_{z_0}^{z_1}(az+c)dz+\int_{z_4}^{z_5}(az+c)dz\right]-\int_{z_0}^{z_1}\lambda_p(az+c)dz \\ &\quad -\int_{z_1}^{z_2}\lambda_{1c}(az+c)dz-\int_{z_2}^{z_3}\lambda_{2c}(az+c)dz-\int_{z_3}^{z_4}\lambda_{1c}(az+c)dz-\int_{z_4}^{z_5}\lambda_p(az+c)dz \\ &= \left(\frac{e_{31}p_3}{\varepsilon_{33}}-\lambda_p\right)\left[\int_{z_0}^{z_1}(az+c)dz+\int_{z_4}^{z_5}(az+c)dz\right] \\ &\quad -\lambda_{1c}\int_{z_1}^{z_2}(az+c)dz-\lambda_{2c}\int_{z_2}^{z_3}(az+c)dz-\lambda_{1c}\int_{z_3}^{z_4}(az+c)dz, \end{aligned} \tag{14a}$$

and

$$\begin{aligned} &z_0=-\frac{3}{2}h_2-h_1,\ z_1=-\frac{3}{2}h_2,\ z_2=-\frac{1}{2}h_2, \\ &z_3=\frac{1}{2}h_2,\ z_4=\frac{3}{2}h_2,\ z_5=\frac{3}{2}h_2-h_1. \end{aligned} \tag{14b}$$

Note that this thermal force is also primarily contributed by the in-plane membrane force $N_{\alpha\alpha}$.

The above derivations of generalized modal forces suggest that for a simply-supported cylindrical shell whose modes are symmetric or anti-symmetric with respect to a line or lines of symmetry, none of the anti-symmetric modes is excited by any of the uniformly distributed mechanical loads, electric loads, or thermal loads. Accordingly, these even modes are filtered from the total response and only the modes that are combinations of $m=1, 3, 5, \cdots$ and $n=1, 3, 5, \cdots$ participate in dynamic response of the cylindrical shell.

3.4. Time responses

There are two time responses considered here: 1) a step response and 2) an impulse response. The step excitation can be considered as a sudden applied constant load and the impulse excitation as a "shock" input. These analytical solutions are presented next.

If these excitations are in the form of step inputs, the individual modal participation factor is determined by

$$\eta_{mn,st}^{i}(t)=\frac{F_{mn}^{i}}{\omega_{mn}^{2}}\left[1-e^{-\zeta_{mn}\omega_{mn}t}\left(\cos(\tilde{\omega}_{mn}t)+\frac{\zeta_{mn}}{\sqrt{1-\zeta_{mn}^{2}}}\sin(\tilde{\omega}_{mn}t)\right)\right], \tag{15}$$

where i is either m (mechanical), c (electric), or t (thermal); and $\tilde{\omega}_{mn}$ is the damped natural frequency $\tilde{\omega}_{mn}=\omega_{mn}\sqrt{1-\zeta_{mn}^{2}}$. Note that the laminated cylindrical shell is assumed under-damped. On the other hand, the modal impulse response to an impulse excitation is

$$\eta_{mn,im}^{i}(t)=\frac{F_{mn}^{i}}{\tilde{\omega}_{mn}}e^{-\zeta_{mn}\omega_{mn}t}\sin(\tilde{\omega}_{mn}t),\quad i=m,\ c,\ t. \tag{16}$$

Detailed response patterns of the cylindrical shell are presented next. Spatially filtered responses are also investigated.

4. Numerical example

In this section, a numerical example is provided to demonstrate the multi-field responses of a laminated cylindrical shell composite. As discussed previously, the laminated composite is made of five laminae: the top and bottom laminae are piezoelectric materials and the middle three laminae are made of graphite/epoxy with 90°/0°/90° lamination. The piezoelectric materials are lead zirconate titanate (PZT) piezoceramics. The laminated shell is 0.1m long in the x direction and 90° curvature angle in the circumferential direction β, its radius R of the middle surface is 0.05m. The thickness of each lamina is 0.0005m. Detailed material properties are listed in Table 1.

It is assumed that the cylindrical shell is simply supported on all four edges and the transverse oscillations are of primary interest. The transverse mode shape function is $U_{3mn}=\sin\frac{m\pi x}{L}\sin\frac{n\pi\alpha}{\beta}$. Natural frequencies of the shell are calculated analytically and numerically (finite element analysis), and these two results are compared favorably. The first sixteen natural frequencies are summarized in Table 2.

Table 1 Material Properties

PZT:	
Young's modulus	$Y_x = Y_y = Y_z = 61$ GPa
Shear modulus	$G_{xy} = G_{xz} = G_{yz} = 23.64$ GPa
Poisson's ratio	$\mu = 0.29$
Density	$\rho = 7.7 \times 10^3$ kg/m^3
Thermal expansion coefficient	$\alpha = 1.2 \times 10^{-6}$ m/m/℃
Electric permittivity	$\varepsilon_{33} = 1.65 \times 10^{-8}$ F/m
Piezoelectric contant	$d_{31} = 171 \times 10^{-12}$ C/N (m/V); $e_{31} = 10.43$ C/m^2
Pyroelectric constant	$p_3 = 0.25 \times 10^{-4}$C/m^2/℃
Graphite/epoxy;	
Young's modulus	$Y_x = 181$ GPa, $Y_y = Y_z = 10.3$ GPa
Shear modulus	$G_{yz} = 2.87$ GPa, $G_{xy} = G_{xz} = 7.17$ GPa
Poisson's ratio	$\mu_{yz} = 0.33$, $M_{xy} = M_{xz} = 0.28$
Density	$\rho = 1.6 \times 10^3$ kg/m^3
Thermal expansion coefficients	$\alpha_1 = 0.02 \times 10^{-6}$ m/m/℃ $\alpha_2 = 22.5 \times 10^{-6}$ m/m/℃

Table 2 Transverse natural frequencies f_{3mn}(Hz)

n/m	1	2	3	4
1	3707.6	7805.1	10958.6	13790.9
2	3868.8	6089.6	9065.6	12476.4
3	8158.2	9412.7	11672.5	14811.0
4	14478.9	15519.7	17414.6	20209.7

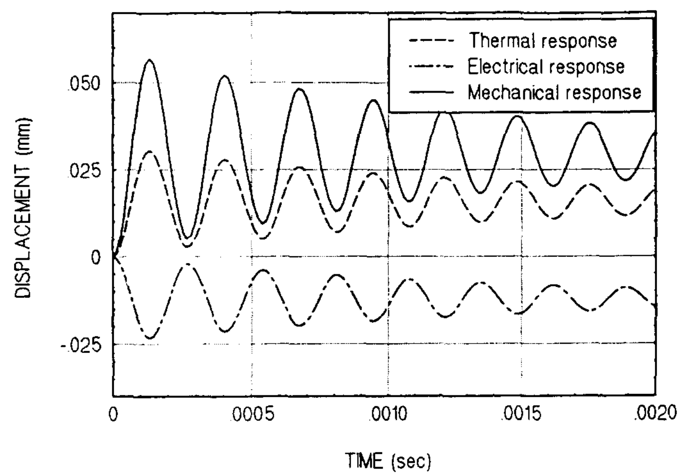

Fig. 3 Multi-field step response of the (1,1) mode.

It is assumed that the mechanical excitation magnitude $q_3^* = 1.0 \times 10^5$(N/m^2)$=0.1$ MPa; electric excitation magnitude $\phi^* = 100$(V); and temperature excitation magnitude $\theta^* = 10$(℃); the time function is a step function and an impulse function. The temperature rise is assumed uniformly distributed in the composite. The modal damping ratio $\zeta_{mn} = 0.03$. Since system is linear, the

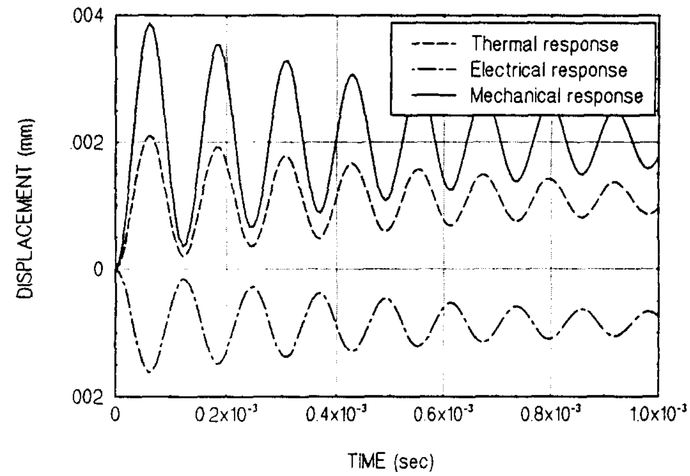

Fig. 4 Multi-field step response of the (1,3) mode.

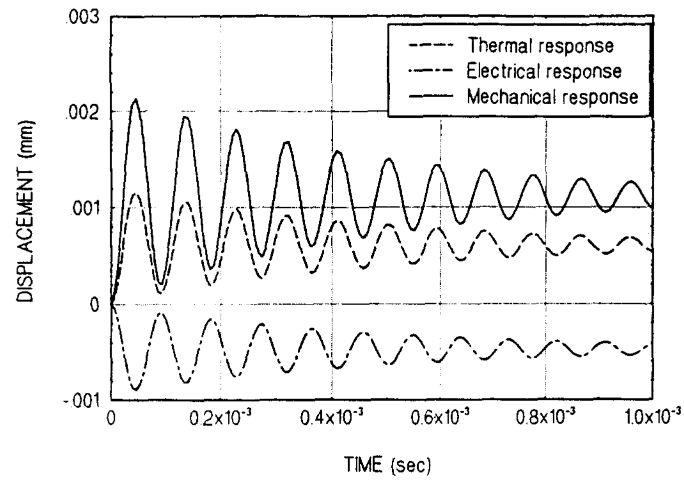

Fig. 5 Multi-field step response of the (3,1) mode.

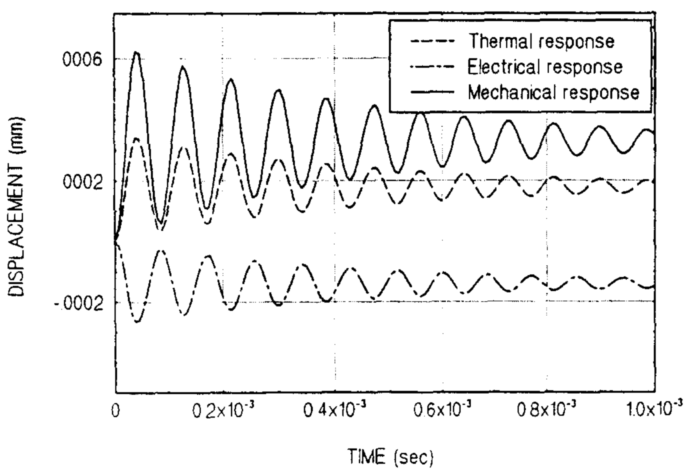

Fig. 6 Multi-field step response of the (3,3) mode.

modal equation becomes

$$\ddot{\eta}_{mn}+2\zeta_{mn}\,\omega_{mn}\,\dot{\eta}_{mn}+\omega_{mn}^{2}\,\eta_{mn}=F_{mn}^{m}(t)+F_{mn}^{c}(t)+F_{mn}^{t}(t). \tag{17}$$

Accordingly, one can calculate the individual modal response $\eta_{mn}^{m}(t)$, $\eta_{mn}^{c}(t)$, and $\eta_{mn}^{t}(t)$ due to its mechanical, electric, and thermal load, respectively. The overall modal response becomes

$$u_3(x,\ \alpha,\ t)=\sum_m\sum_n \eta_{mn}(t)U_{3mn}(x,\ \alpha)=\sum_m\sum_n[\eta_{mn}^{m}(t)+\eta_{mn}^{c}(t)+\eta_{mn}^{t}(t)]U_{3mn}(x,\ \alpha). \tag{18}$$

Note that the response $u_3(x,\ \alpha,\ t)$ is a spatial function. As long as the total solution is determined, the multi-field displacement response of any location can be calculated easily. The individual responses of these component excitations are calculated and plotted to show their respective contributions. The total response is a summation of all these individual responses. Multi-field step and impulse responses of the laminated cylindrical shell are presented below.

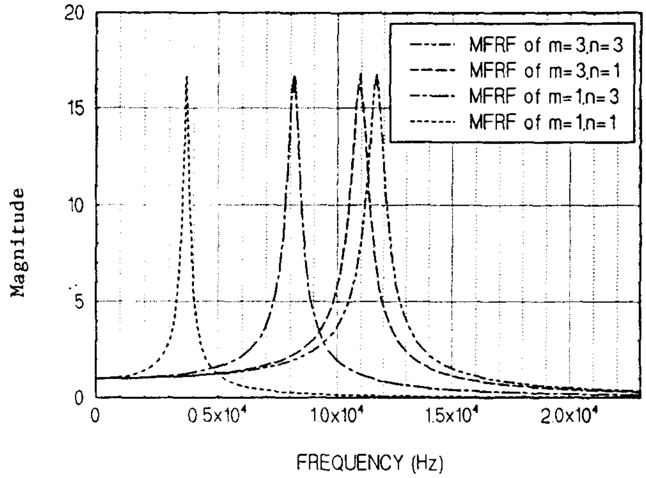

Fig. 7 Magnitude responses.

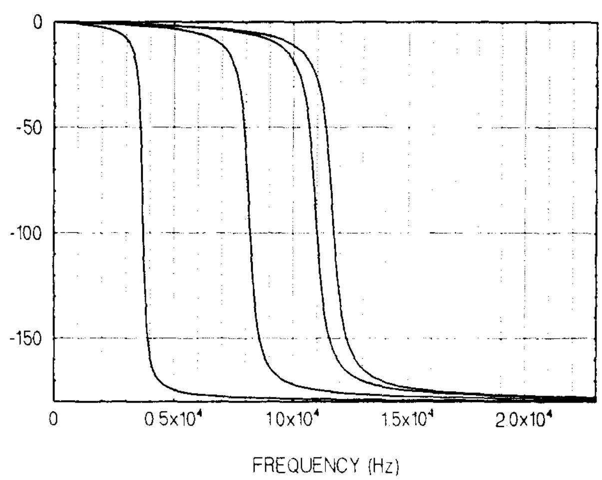

Fig. 8 Phase responses.

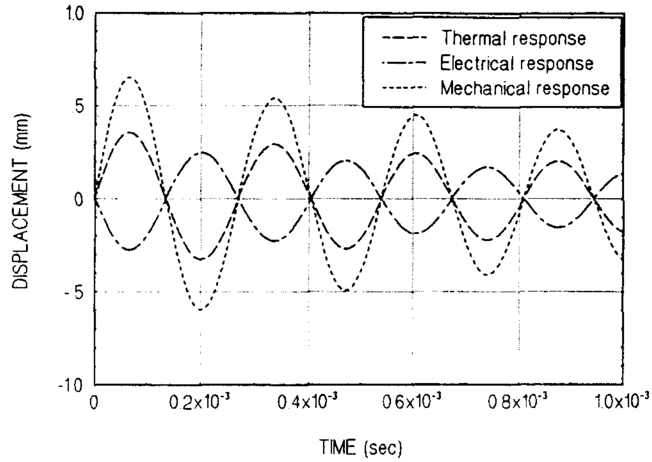

Fig. 9 Multi-field impulse response of the (1,1) mode.

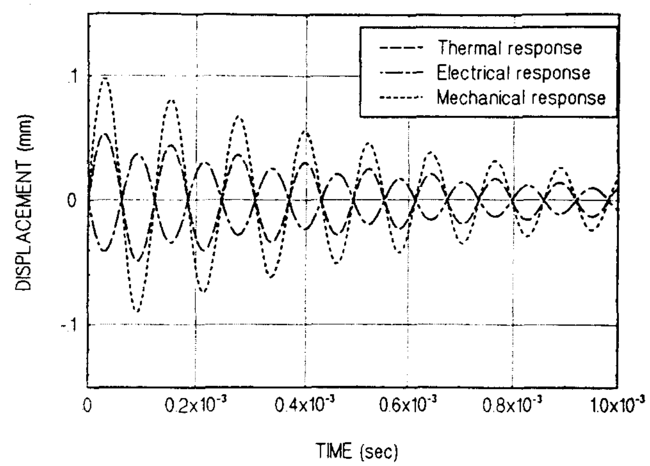

Fig. 10 Multi-field impulse response of the (1,3) mode.

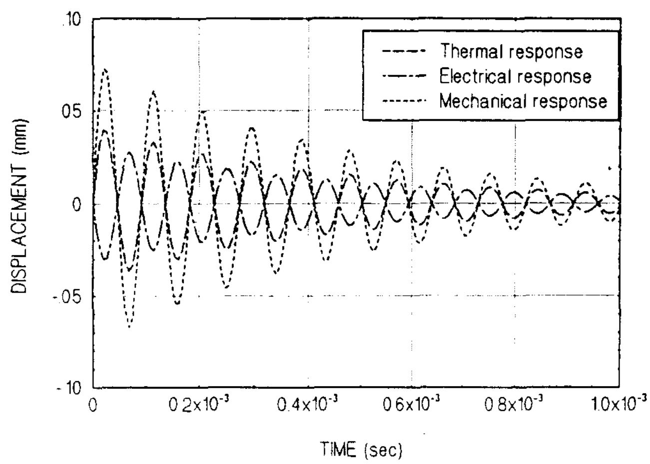

Fig. 11 Multi-field impulse response of the (3,1) mode.

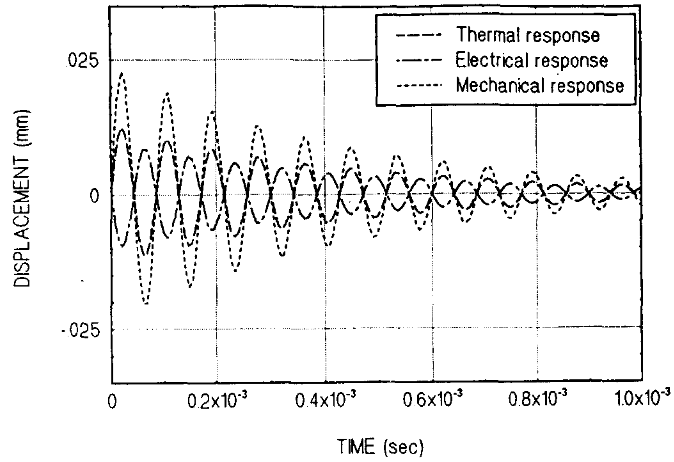

Fig. 12 Multi-field impulse response of the (3,3) mode.

4.1 Multi-field step responses

Figs. 3 to 6 illustrate the step time-history responses of the (1,1), (1,3), (3,1), and (3,3) modes. (Recall that all even modes are not excited due to their spatial characteristics.) The mechanical and thermal induced displacements are in phase, and the electric induced displacement is out-of-phase. Accordingly, the electric excitation can be used to control the mechanical and thermal induced excitations. Magnitude of the modal frequency response functions of these natural modes are plotted in Fig. 7; their phase responses are plotted in Fig. 8. Since the initial modal damping ratios are assumed the same, they all have very similar responses.

4.2 Multi-field impulse responses

Figs. 9 to 12 illustrates of the multi-field impulse responses of the first four odd modes, i.e., the (1,1), (1,3), (3,1), and (3,3) modes. As discussed previously, the mechanical and thermal induced oscillations are in phase, and the electric induced oscillation is out-of-phase. Accordingly, the electric excitation can be used to compensate the mechanical and thermal induced oscillations.

5. Discussion and conclusion

External temperature fluctuation can significantly change the piezoelectric and control characteristics of piezoelastic structures. In this paper, multi-field step and impulse responses of a laminated piezothermoelastic cylindrical shell composite were studied and spatially filtered phenomena were investigated.

Generic solution procedures of piezothermoelastic shells subjected to mechanical, electric, and temperature excitations were presented first. Detailed definitions of their spatial and time components were discussed afterwards. The spatial function was assumed uniformly distributed and the time functions were a step function and an impulse function, respectively. Analytical derivations suggested that the uniformly distributed excitation can only excite odd modes, and are ineffective to all even modes. Accordingly, these even modes are filtered from the total response. Since the system is linear, the total response is a summation of all participating modal responses.

Multi-field step and impulse responses of the laminated cylindrical shell laminate showed that the displacements induced by mechanical and temperature excitations are in phase, and that induced by the electric execitation is out-of-phase. Accordingly, the electric excitation can be used to compensate the mechanical and temperature induced excitations, and accordingly active vibration control can be successfully achieved.

Acknowledgement

This research was supported by a grant from the Army Research offce (DAAL03-91-G-0065), Technical Monitor: Dr. Gary L. Anderson. Contents of the information do not necessarily reflect the position or the policy of the government, and nor should official endorsement be inferred.

References

Mindlin, R. D. (1974), "Equations of high frequency vibrations of thermopiezoelectric crystal plates," *Intl. J. Solids and Structures*, **10**, 625-637.

Nowacki, J. P. (1982), "Steady-state problems of thermopiezoelectricity," *Journal of Thermal Stress*, **5**, 183-194.

Nowacki, W. (1978), "Some general theorems of thermopiezoelectricity," *Journal of Thermal Stress*, **1**, 171-182.

Soedel, W (1993), *Vibrations of shells and plates*, Marcer-Dekker, New York.

Tzou, H. S. (1993), *Piezoelectric Shells (Distributed Sensing and Control of Continua)*, Kluwer Academic Publishers, Boston/Dordrecht.

Tzou, H. S. and Anderson, G. L. (1992), *Intelligent Structural Systems*, Kluwer Academic Publishers, Boston/Dordrecht.

Tzou, H. S. and Bao, Y. (1995a), "A theory on anisotropic piezothermoelastic shell laminae with sensor and actuator applications," *Journal of Sound and Vibration* **184**(3), 453-473.

Tzou, H. S. and Bao, Y. (1995b), "Dynamics and control of adaptive shells with curvature transformations" *Shock and Vibration Journal*, **2**(2), 143-154.

Tzou, H. S. and Fukuda, T. (1992), *Precision Sensors, Actuators and Systems*, Kluwer Academic Publishers, Boston/Dordrecht.

Tzou, H. S. and Howard, R. V. (1994a), "A piezothermoelastic shell theory applied to active structures," *ASME* Transactions *Journal of Vibration and Acoustics*, **116**(3) 295-302.

Tzou, H. S. and Howard, R. V., (1994b), "Distributed control of a circular ring subjected to mechanical and thermal excitations," *SPIE* Paper No. 2190-81, 1994 *SPIE North American Conference on Smart Structures and Materials*, Orlando, F. L, February 13-18, 1994.

Tzou, H. S. and Ye, R. (1994), "Piezothermoelasticity and precision control of piezoelectric laminates: Theory and finite element analysis," *ASME Journal of Vibration and Acoustics*, **116**(4), 489-495.

Appendix

Operators of generic piezothermoelastic shells

Mechanical Love's operators $L_i^m\{u_1, u_2, u_3\}$ are defined as

$$L_1^m\{u_1, u_2, u_3\}=\frac{1}{A_1A_2}\left\{\frac{\partial(N_{11}^m A_2)}{\partial\alpha_1}-N_{22}^m\frac{\partial A_2}{\partial\alpha_1}+\frac{\partial(N_{12}^m A_1)}{\partial\alpha_2}+N_{12}^m\frac{\partial A_1}{\partial\alpha_2}\right.$$
$$\left.+\frac{1}{R_1}\left[\frac{\partial(M_{11}^m A_2)}{\partial\alpha_1}-M_{22}^m\frac{\partial A_2}{\partial\alpha_1}+\frac{\partial(M_{12}^m A_1)}{\partial\alpha_2}+M_{12}^m\frac{\partial A_1}{\partial\alpha_2}\right]\right\}, \tag{A1}$$

$$L_2^m\{u_1, u_2, u_3\}=\frac{1}{A_1A_2}\left\{\frac{\partial(N_{12}^m A_2)}{\partial\alpha_1}+N_{12}^m\frac{\partial A_2}{\partial\alpha_1}+\frac{\partial(N_{22}^m A_1)}{\partial\alpha_2}-N_{11}^m\frac{\partial A_1}{\partial\alpha_2}\right.$$
$$\left.+\frac{1}{R_2}\left[\frac{\partial(M_{12}^m A_2)}{\partial\alpha_1}+M_{12}^m\frac{\partial A_2}{\partial\alpha_1}+\frac{\partial(M_{22}^m A_1)}{\partial\alpha_2}-M_{11}^m\frac{\partial A_1}{\partial\alpha_2}\right]\right\}, \tag{A2}$$

$$L_3^m\{u_1, u_2, u_3\}=\frac{1}{A_1A_2}\left\{\frac{\partial}{\partial\alpha_1}\left[\frac{1}{A_1}\left(\frac{\partial(M_{11}^m A_2)}{\partial\alpha_1}-M_{22}^m\frac{\partial A_2}{\partial\alpha_1}+\frac{\partial(M_{12}^m A_1)}{\partial\alpha_2}+M_{12}^m\frac{\partial A_1}{\partial\alpha_2}\right)\right]\right.$$
$$+\frac{\partial}{\partial\alpha_2}\left[\frac{1}{A_2}\left(\frac{\partial(M_{12}^m A_2)}{\partial\alpha_1}+M_{12}^m\frac{\partial A_2}{\partial\alpha_1}+\frac{\partial(M_{22}^m A_1)}{\partial\alpha_2}-M_{11}^m\frac{\partial A_1}{\partial\alpha_2}\right)\right]$$
$$\left.-A_1A_2\left(\frac{N_{11}^m}{R_1}+\frac{N_{22}^m}{R_2}\right)\right\}, \tag{A3}$$

where N_{ij}^m are the elastic membrane forces; M_{ij}^m are the elastic bending moments; A_1 and A_2 are the Lamé parameters; R_1 and R_2 are the radii of curvatures (Tzou 1993). Operators of the direct piezoelectric effect $L_i^d\{u_1, u_2, u_3\}$ are defined as

$$L_1^d\{u_1, u_2, u_3\}=-\frac{1}{A_1A_2}\left\{\frac{\partial(N_{11}^d A_2)}{\partial\alpha_1}-N_{22}^d\frac{\partial A_2}{\partial\alpha_1}+\frac{\partial(N_{12}^d A_1)}{\partial\alpha_2}+N_{12}^d\frac{\partial A_1}{\partial\alpha_2}\right.$$
$$\left.+\frac{1}{R_1}\left[\frac{\partial(M_{11}^d A_2)}{\partial\alpha_1}-M_{22}^d\frac{\partial A_2}{\partial\alpha_1}+\frac{\partial(M_{12}^d A_1)}{\partial\alpha_2}+M_{12}^d\frac{\partial A_1}{\partial\alpha_2}\right]\right\}, \tag{A4}$$

$$L_2^d\{u_1, u_2, u_3\}=-\frac{1}{A_1A_2}\left\{\frac{\partial(N_{12}^d A_2)}{\partial\alpha_1}+N_{12}^d\frac{\partial A_2}{\partial\alpha_1}+\frac{\partial(N_{22}^d A_1)}{\partial\alpha_2}-N_{11}^d\frac{\partial A_1}{\partial\alpha_2}\right.$$
$$\left.+\frac{1}{R_1}\left[\frac{\partial(M_{12}^d A_2)}{\partial\alpha_1}+M_{12}^d\frac{\partial A_2}{\partial\alpha_1}+\frac{\partial(M_{22}^d A_1)}{\partial\alpha_2}-M_{11}^d\frac{\partial A_1}{\partial\alpha_2}\right]\right\}, \tag{A5}$$

$$L_3^d\{u_1, u_2, u_3\}=-\frac{1}{A_1A_2}\left\{\frac{\partial}{\partial\alpha_1}\left[\frac{1}{A_1}\left(\frac{\partial(M_{11}^d A_2)}{\partial\alpha_1}-M_{22}^d\frac{\partial A_2}{\partial\alpha_1}+\frac{\partial(M_{12}^d A_1)}{\partial\alpha_2}+M_{12}^d\frac{\partial A_1}{\partial\alpha_2}\right)\right]\right.$$
$$+\frac{\partial}{\partial\alpha_2}\left[\frac{1}{A_2}\left(\frac{\partial(M_{12}^d A_2)}{\partial\alpha_1}+M_{12}^d\frac{\partial A_2}{\partial\alpha_1}+\frac{\partial(M_{22}^d A_1)}{\partial\alpha_2}-M_{11}^d\frac{\partial A_1}{\partial\alpha_2}\right)\right]$$
$$\left.-A_1A_2\left(\frac{N_{11}^d}{R_1}+\frac{N_{22}^d}{R_2}\right)\right\}, \tag{A6}$$

where N_{ij}^d are the electric membrane forces; M_{ij}^d are the electric bending moments. Both of them are induced by the piezoelectric effect (Tzou 1993). Operators of the converse piezoelectric effect $L_i^c\{\phi_3\}$ can be defined by replacing all superscript "d" by "c" in Eqs. (A4)-(A6). Similarly, one can define operators of the pyroelectric effect $L_i^p\{\theta\}$ and operators of the temperature effect $L_i^\theta\{\theta\}$. α_1, α_2 and α_3 are the three coordinates in the curvilinear coordinate system.